Biochimica et Biophysica Acta 1837 (2014) 1944–1954

Contents lists available at ScienceDirect

Biochimica et Biophysica Acta

journal homepage: www.elsevier.com/locate/bbabio

Non-photochemical reduction of thylakoid photosynthetic redox carriers in vitro: Relevance to cyclic electron flow around photosystem I?

Nicholas Fisher [a], David M. Kramer [a,b,*]

[a] MSU-DOE Plant Research Laboratory, Michigan State University, East Lansing, MI 48824, USA
[b] Department of Biochemistry and Molecular Biology, Michigan State University, East Lansing, MI 48824, USA

ARTICLE INFO

Article history:
Received 23 May 2014
Received in revised form 7 September 2014
Accepted 14 September 2014
Available online 22 September 2014

Keywords:
Photosynthesis
Chlorophyll fluorescence
Cyclic electron flow
Photosystem II
PGR5
Plastoquinone

ABSTRACT

Non-photochemical (dark) increases in chlorophyll *a* fluorescence yield associated with non-photochemical reduction of redox carriers (F_{npr}) have been attributed to the reduction of plastoquinone (PQ) related to cyclic electron flow (CEF) around photosystem I. In vivo, this rise in fluorescence is associated with activity of the chloroplast plastoquinone reductase (plastid NAD(P)H:plastoquinone oxidoreductase) complex. In contrast, this signal measured in isolated thylakoids has been attributed to the activity of the protein gradient regulation-5 (PGR5)/PGR5-like (PGRL1)-associated CEF pathway. Here, we report a systematic experimentation on the origin of F_{npr} in isolated thylakoids. Addition of NADPH and ferredoxin to isolated spinach thylakoids resulted in the reduction of the PQ pool, but neither its kinetics nor its inhibitor sensitivities matched those of F_{npr}. Notably, F_{npr} was more rapid than PQ reduction, and completely insensitive to inhibitors of the PSII Q_B site and oxygen evolving complex as well as inhibitors of the cytochrome b_6f complex. We thus conclude that F_{npr} in isolated thylakoids is not a result of redox equilibrium with bulk PQ. Redox titrations and fluorescence emission spectra imply that F_{npr} is dependent on the reduction of a low potential redox component (E_m about −340 mV) within photosystem II (PSII), and is likely related to earlier observations of low potential variants of Q_A within a subpopulation of PSII that is directly reducible by ferredoxin. The implications of these results for our understanding of CEF and other photosynthetic processes are discussed.

1. Introduction

Oxygenic photosynthesis involves light-driven electron transfer reactions that reduce and re-oxidise plastoquinone (PQ), a lipophilic molecule located within the thylakoid membranes of cyanobacteria and chloroplasts. These redox reactions are coupled to proton uptake and release that establish an electrochemical gradient of protons, the Gibbs energy of which is harnessed to drive the endergonic ATP synthesis reactions of the (C)F_1–(C)F_o ATP synthase [1,2].

Electrons participating in the light-dependent reactions of oxygenic photosynthesis may either follow a linear pathway (linear electron flow, LEF) from water to NADP+ requiring photosystem I (PSI) and photosystem II (PSII) to operate in a concerted manner, or by a cyclic electron flow (CEF) pathway around photosystem I (PSI) in which ferredoxin (Fd) serves to re-reduce the PQ pool without NADPH generation or water oxidation.

In green plants, LEF translocates six protons per two electrons ($6H^+/2e$) transferred from water to NADP+, which coupled with an (C)F_1-(C)F_o ATP synthase containing 14 proton-binding c-subunits (4.67 H^+/ATP), generates 2.6 molecules of ATP per 2 molecules of NADPH. This is insufficient for sustained operation of the Calvin–Benson–Bassham (CBB) cycle, which requires an ATP:NADPH ratio of 3:2. The CEF pathway has capability to redress this energetic imbalance [3]. In addition, CEF, via its protonmotive activity, may contribute to the photoprotective energy-dependent non-photochemical quenching pathway, qE [4,5].

Despite intensive investigation, the physiological significance and molecular enzymology of CEF remain unclear [6–9]. In higher plants, there are at least two pathways for CEF that may operate in parallel or differentially in different tissues or metabolic states [9]. One of these involves the plastid NAD(P)H:plastoquinone oxidoreductase (NDH) complex, a homologue of mitochondrial respiratory Complex I [10,11]. A second pathway involves an antimycin A-sensitive PQ reductase [12–14]. Latterly, this pathway has been proposed to involve the *protein gradient regulation-5* (PGR5) protein, identified by Munekage et al. [15] through a mutant screen of *Arabidopsis thaliana*. PGR5 is a small

Abbreviations: AA, antimycin A; ADRY, *a*cceleration of the *d*eactivation *r*eactions of the water-splitting enzyme system *Y*; CEF, cyclic electron flow (around photosystem I); DCMU, 3-(3,4-Dichlorophenyl)-1,1-dimethylurea; DPI, diphenylene iodonium chloride; Fd, ferredoxin; F_{npr}, chlorophyll *a* *f*luorescence yield increase associated with *n*on-photochemical *r*eduction of redox carriers; FNR, ferredoxin:$NADP^+$ reductase; HA, hydroxylamine; NDH, plastid NAD(P)H:plastoquinone oxidoreductase; PQ, plastoquinone; PS I, photosystem I; PS II, photosystem II; TDS, tridecylstigmatellin

* Corresponding author at: MSU-DOE Plant Research Laboratory, Michigan State University, East Lansing, MI 48824, USA. Tel.: +1 517 432 0072.
E-mail address: kramerd8@msu.edu (D.M. Kramer).

http://dx.doi.org/10.1016/j.bbabio.2014.09.005
0005-2728/

(10 kDa), soluble and highly basic protein with no recognisable electron transfer functionality. The PRGL1 protein was found to interact with PGR5 and be required for CEF activity [16], and this complex has been proposed [17] to directly act as the plastoquinone reductase in an in vitro reconstituted system. The relative contributions of these two pathways to the CEF pathway remain controversial [9,18–21].

Both NDH- and PRG5-associated pathways have been probed using the chlorophyll fluorescence rise observed after cessation of a period of steady-state illumination, or, alternatively, as observed on the addition of Fd and NADPH to osmotically ruptured chloroplast preparations. This rise has been generally accepted to originate from the non-photochemical reduction of plastoquinone associated with CEF or chlororespiration [10,22–26]. Here we refer to this phenomenon as F_{npr}, for fluorescence change associated with non-photochemical reduction. The F_{npr} signal in vivo was successfully used to screen for a large number of mutants affected in the assembly and activity of the NDH [7,27,28] establishing a clear link between this signal and the NDH-associated CEF pathway. Curiously, though, F_{npr} in isolated thylakoids has largely been ascribed to the activity of the PGR5-associated PQ reductase, with only smaller contributions from NDH [15,16,29,30], suggesting that NDH and PGR5 activities are differentially lost upon thylakoid isolation.

Adding to the uncertainty, it has not yet been established experimentally that F_{npr} signal actually reflects the reduction of PQ under all conditions, and a number of questions have arisen about the interpretation of F_{npr}. It has been noted that the rate of PQ reduction inferred from F_{npr} (which can exhibit a half-time of tens of seconds) is too slow to be compatible with CEF in vivo [19,23,26], with a CEF electron transfer turnover rate of 16–20 $e^- s^{-1}$ required during a steady state LEF rate of 150 $e^- s^{-1}$, assuming an H^+/ATP stoichiometry of 4.67 [31]. Only a minor fraction (5–10%) of Q_A is observed to be reducible on Fd + NADPH addition in the F_{npr} assay, despite a strongly favourable energetic driving force [32]. Mutation of the gene encoding for the PGR5 protein affects the amplitude of the F_{npr} signal, but does not affect its half-time, in apparent contradiction with the proposed role in reducing bulk plastoquinone [15,29]. Some of the effects of *pgr5* can also be explained by chloroplast ATP synthase activity rather than CEF [18].

To address these open questions, we systematically re-examined the physical and biochemical basis of the F_{npr} in spinach chloroplast preparations in an attempt to resolve some of the controversies concerning the applicability of this method to the investigation of CEF.

2. Materials and methods

2.1. Reagents, plant material, Fd purification and chloroplast isolation

Reagents were purchased from Sigma-Aldrich (St Louis, MO) unless otherwise noted. Tridecylstigmatellin was generously supplied by Prof. Paul O'Neill (University of Liverpool, UK). Spinach was purchased from a local market.

Spinach Fd was isolated using a modification of the method of Plesnicar and Bendall [33]. Briefly, supernatant from the dialysed spinach leaf acetone precipitate was applied to a 2.5 × 15 cm DE-Sepharose FPLC column equilibrated with 25 mM HEPES (pH 7.6). The column was washed with two volumes of equilibration buffer and the Fd eluted with a linear five-column volume 0–0.5 M NaCl gradient in equilibration buffer at a flow rate of 1.0 ml min^{-1}. All chromatographic steps were performed at 4 °C. Fd-containing fractions were identified visually and concentrated using Amicon 'Ultra' centrifugal concentrators (Millipore, 10 kDa cut-off). The Fd was quantitated spectrophotometrically (ε_{420} = 9.7 mM^{-1} cm^{-1}[34]) and used without further purification.

Spinach chloroplasts were prepared according to a modified version of the procedure of Seigneurin-Berny et al. [35]. Using a domestic blender, approximately 20 g of leaves was homogenised for 10 s in ice-cold grinding medium consisting of 50 mM HEPES (pH 7.6), 330 mM sorbitol, 5 mM $MgCl_2$, 2 mM EDTA, 10 mM ascorbate and 0.1% (w/v) BSA. The crude extract was passed through a wetted filter consisting of one layer of muslin and a layer of Miracloth prior to centrifugation at 4000 ×*g* for 5 min (4 °C). The chloroplast pellet was resuspended in a minimal volume (<1 ml) of osmotic lysis buffer (10 mM HEPES, 10 mM $MgCl_2$, pH 7.6) and chlorophyll quantitated in 80% (v/v) acetone using the method of Inskeep and Bloom [36].

Hydroxylamine was prepared fresh daily as a 100 mM solution (pH adjusted to 7.6 with sodium hydroxide) and kept on ice.

2.2. Kinetic spectrofluorimetry and the NADPH-linked chlorophyll fluorescence rise assay

Chlorophyll fluorescence from osmotically ruptured chloroplast suspensions was measured in a laboratory-constructed kinetic spectrofluorometer modified to use cuvette-based samples with optics and electronics based on those described elsewhere [37]. Chlorophyll fluorescence was excited by weak pulses of BG-18 filtered (Edmund Optics, Barrington, NJ) light from a 505 nm LED source (Luxeon). The measuring pulse frequency was 1 Hz and the intensity 0.1 μmol photons m^{-2} s^{-1}. Actinic light was provided by a red LED (620 nm). Far-red fluorescence emission was transmitted through a RG-9 filter (Edmund Optics) and measured perpendicularly to the path of the measuring- and actinic sources.

The F_{npr} assay was measured using osmotically ruptured spinach chloroplasts at a chlorophyll concentration of 20 μg ml^{-1} in osmotic lysis buffer (10 mM HEPES, 10 mM $MgCl_2$, pH 7.6), supplemented with 5 μM spinach Fd. The reaction was initiated by the addition of 100 μM NADPH, and all measurements were performed at room temperature (21 °C). DCMU and hydroxylamine, when used, were present at 10 μM and 1 mM respectively. Hydroxylamine was added immediately prior to the start of data collection to minimise the possibility of damage to the PSII oxygen evolving complex.

2.3. Redox titration of the NADPH-associated chlorophyll fluorescence rise

Redox titration of the F_{npr} in osmotically ruptured spinach chloroplasts (20 μg Chl ml^{-1}) was performed by manipulation of the NADPH:$NADP^+$ molar ratio (at a constant NADPH concentration of 100 μM) in lysis buffer supplemented with 5 μM Fd in the kinetic spectrofluorometer setup described above. The redox titration was performed under aerobic- and anaerobic conditions. Anoxia was achieved by deoxygenating the lysis buffer (in a 4 ml cuvette sealed with a silicone septum) with a gentle stream of nitrogen for 10 min prior to the start of the experiment. The redox titration was performed under a nitrogen-filled headspace within the cuvette, with reagents introduced by a Hamilton syringe. Additionally, glucose (1 mM), glucose oxidase (1 μg ml^{-1}) and catalase (1 μg ml^{-1}) were included in the lysis buffer for the redox titration performed under anaerobic conditions. NADPH and $NADP^+$ were prepared at a nominal concentration of 100 mM in double distilled water and quantitated spectrophotometrically (NADPH: ε_{340} = 6.22 mM^{-1} cm^{-1}, NADP+: ε_{260} = 16.9 mM^{-1} cm^{-1}) prior to dilution into lysis buffer (pH 7.6) to form 10 mM working solutions for use in the redox titration. During the titration, the ambient redox potential (corrected for pH 7.6) was calculated using the Nernst equation assuming $E_{m,7}$ (NADPH / $NADP^+$) = −320 mV.

2.4. FNR activity assay

Spinach FNR activity was measured spectrophometrically as NADPH-associated Fd:cytochrome *c* reductase activity at 550*minus* 542 nm in a laboratory constructed spectrophotometer at 21 °C. Spinach FNR was purchased from Sigma-Aldrich and used without further purification. The reaction medium consisted of 50 mM

potassium phosphate (pH 7.5), 2 mM EDTA, 5 μM spinach Fd, 20 μM equine heart cytochrome *c* and 0.02 units of spinach FNR (approximately 1.5 μg). The reaction was initiated by the addition of 100 μM NADPH, and kinetic data were collected for 4 min. Rates were measured by straight-line fits to the initial 20 s after NADPH addition, using $\varepsilon_{550-542} = 18.5\ mM^{-1}\ cm^{-1}$[38]. The non-enzymatic rate of cytochrome *c* reduction in the presence of NADPH and Fd was negligible. Antimycin A and diphenyleneiodonium chloride (DPI) were prepared as 10 mM ethanolic- and DMSO stocks respectively.

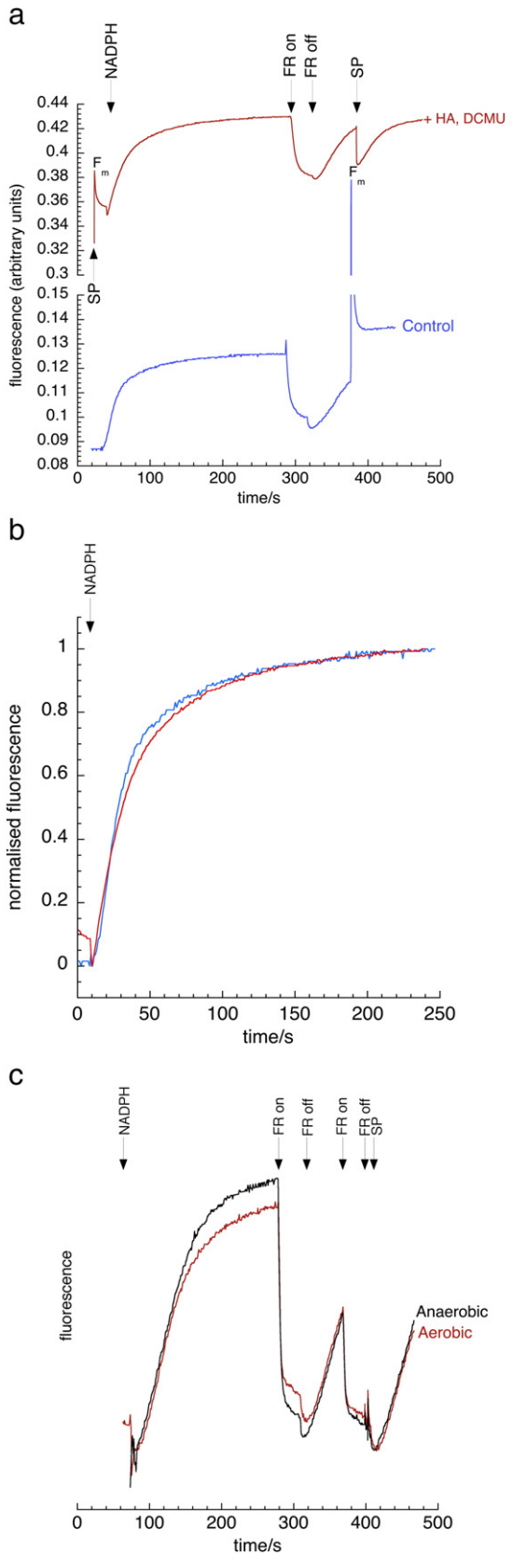

Fig. 1. (a). F_{npr} in osmotically ruptured spinach chloroplasts (20 μg Chl ml^{-1}) in the presence (red) and absence (blue) of 1 mM hydroxylamine and 10 μM DCMU. The fluorescence rise was initiated by the addition of 100 μM NADPH. Saturating actinic pulses (620 nm) are indicated by 'SP' (note that the initial saturating pulse prior to the addition of NADPH was not applied in the experiment performed in the absence of HA and DCMU). The period of illumination by far-red light is indicated by 'FR on' and 'FR off'. Maximal fluorescence is indicated by 'F_m'. The assay buffer consisted of 10 mM HEPES (pH 7.6), 10 mM $MgCl_2$, 5 μM Fd. (b) Normalisation of the F_{npr} hyperbola presented in (a). Blue- and red-kinetic data correspond to the control- and HA/DCMU treated samples respectively. (c) The effect of oxygen on F_{npr} in the presence of 1 mM hydroxylamine and 10 μM DCMU. Data are presented for aerobic (red, ambient O_2) and anaerobic (black) conditions. Anoxia was achieved through the use of nitrogen sparging and glucose oxidase activity in a sealed cuvette, as described in Section 2.3. Other conditions and treatments are as in (a). The initial saturating pulse is not shown.

2.5. Room temperature chlorophyll fluorescence emission spectra

Room temperature (21 °C) chlorophyll fluorescence emission spectra were obtained using a laboratory-built spectrofluorometer constructed from a modified Aminco–Bowman spectrophotofluorometer fitted with a 1024 pixel Spectrum CCD detector from Acton Research Corporation (Redmond, WA). The excitation wavelength was 440 nm. CCD exposure time was set to 20 ms per spectrum, with 128 spectra collected per frame. 30 frames were collected per experiment with an 8 s delay between frame collections. Spinach chloroplasts were resuspended in osmotic lysis buffer at a chlorophyll concentration of 20 μg ml^{-1}. Spinach Fd was present at 5 μM. 100 μM NADPH or 10 μM DCMU was introduced to the chloroplasts 90 s after the initiation of data collection as appropriate. Hydroxylamine, when used, was present at a concentration of 1 mM. Hydroxylamine-containing samples were illuminated with red light (620 nm, 200 μmol photons $m^{-2}\ s^{-1}$) for 2 s immediately prior to fluorescence emission spectrum collection. Difference spectra were obtained from the binned averages of four frames of data (512 individual spectra) recorded before- and 2 min after NADPH (or DCMU) addition.

2.6. 77 K chlorophyll fluorescence emission spectra

77 K chlorophyll fluorescence spectra were obtained using an Ocean Optics HR2000 + ES fibre optic spectrometer (Ocean Optics, Dunedin, FL). The excitation source was a 440 nm 5 mW diode laser (World Star Tech, Toronto). Osmotically ruptured spinach chloroplasts were diluted to 4 μg chlorophyll ml^{-1} in osmotic lysis buffer supplemented with 5 μM Fd. 250 μl samples of chloroplasts in this assay buffer were frozen at 77 K in 4 mm internal diameter NMR tubes (Norell) before- and 2 min after the addition of 100 μM NADPH. Difference spectra were calculated from the means of four discrete samples before- and after NADPH addition, with four absolute spectra collected per sample. Using the SpectraSuite software package (Ocean Optics, Dunedin, FL) five scans were averaged per absolute spectrum, using a 100 ms integration time and 5 pixel boxcar smoothing. Difference spectra were averaged and normalised to the emission peak at 694 nm using Kaleidagraph 4.5 (Synergy Software, Reading, PA).

2.7. P_{700} redox spectrophotometry

P_{700} redox changes in osmotically ruptured spinach chloroplasts were monitored in a laboratory-constructed spectrophotometer utilising a pulsed white LED filtered through a 700 nm bandpass filter (10 nm bandwith, Edmund Optics) as the measuring beam source [37]. Actinic light (75 μmol photons $m^{-2}\ s^{-1}$) was provided by a

720 nm bandpass-filtered (10 nm bandwidth, Edmund Optics) white LED situated perpendicularly to the measuring beam.

The assay buffer consisted of osmotic lysis buffer at pH 7.6 supplemented with 5 μM spinach Fd, 10 μM DCMU, 1 mM hydroxylamine and 100 μM NADPH. Chloroplasts were resuspended in this buffer at 40 μg Chl ml^{-1}. All experiments were performed at 21 °C.

3. Results

3.1. Enzymological, spectroscopic and physicochemical properties of the F_{npr}

3.1.1. Chlorophyll fluorescence rise on Fd + NADPH addition in osmotically ruptured chloroplasts

Fig. 1(a) presents the characteristic F_{npr} signal using osmotically ruptured spinach chloroplasts in the presence of 5 μM spinach Fd on addition of 100 μM NADPH. Chlorophyll fluorescence was measured using a weak LED source pulsed with a 1 Hz pulse frequency, 20 μs pulse duration, maximal LED emission at 505 nm, filtered through a BG18 blue-green glass filter (Edmund Optics, Inc.), with integrated intensity less than 0.1 μmol photons m^{-2} s^{-1}. The chloroplasts were osmotically lysed in situ in an aerobic reaction buffer consisting of 10 mM HEPES, 10 mM $MgCl_2$, pH 7.6. The half-time of the F_{npr} was approximately 20 s (corresponding to an apparent first-order rate constant of approximately 0.035 s^{-1}), reaching a maximum level of fluorescence which was 15% of that observed following a saturating actinic pulse (620 nm, 5000 μmol photons m^{-2} s^{-1}, 400 ms duration). No increase in chlorophyll fluorescence was observed when experiments were performed in the absence of either Fd or NADPH (Fig. S1), in accordance with earlier investigations [22,24]. The kinetics of the NADPH/Fd-dependent F_{npr} presented in this study are similar those observed by others in spinach and *A. thaliana* chloroplast preparations [15,22,24,29], with a half-time of approximately 20 s, corresponding to a first order rate constant of approximately 0.035 s^{-1}. A variability of approximately ±5 s was observed in this half-time between chloroplast preparations from different batches of spinach, which presumably arises from variability in the age, growth- and storage conditions of the harvested material. It should be noted that the amplitude of the F_{npr} signal when compared to that of maximal fluorescence yield achieved during a saturating actinic pulse (F_m), suggests that this phenomenon is associated with a minor fraction of PSII; i.e. the bulk of the population of $Q_A$was not reduced on NADPH + Fd addition.

Application of far-red illumination (740 nm, 50 μmol photons m^{-2} s^{-1}) led to quenching the NADPH-induced fluorescence, which recovered to the original level upon removal of the far-red excitation with recovery kinetics identical to that observed for the initial fluorescence rise. The kinetics for the far-red quenching exhibited a half-time of approximately 5 s. Importantly, essentially identical fluorescence quenching- and recovery phenomenology were observed using red (620 nm) illumination (Fig. 1(a)), indicating that the effects were not related to oxidation of PQ by PSI (see also below).

The role of bulk plastoquinone (PQ) in F_{npr} was then investigated in the presence of hydroxylamine (HA, 1 mM) and DCMU (10 μM), conditions under which PSII-associated variable fluorescence and redox equilibration between Q_A and the bulk PQ pool should be eliminated. Hydroxylamine rapidly reduces the oxygen evolving complex (OEC) to the S_1 state, with prolonged incubation resulting in super-reduction ($S_{<0}$) and subsequent manganese loss. Q_A^-/S_1 charge recombination is energetically unfavourable, greatly delaying the quenching of variable fluorescence following a saturating actinic pulse [39–41]. Osmotically-lysed chloroplasts were illuminated with a pulse of red light (5000 μmol photons m^{-2} s^{-1} for 400 ms) after HA/DCMU addition to ensure accumulation of Q_A^- prior to the addition of 100 μM NADPH. In the presence of Fd, addition of NADPH resulted in a 1.3-fold increase in chlorophyll fluorescence yield, above the level of F_m obtained by the saturating pulse in the absence of HA/DCMU. The kinetics of the rise were similar to that observed in the absence of HA/DCMU, with a half-time of approximately 20 s. Further application of saturating pulses (620 nm, 5000 μmol photons m^{-2} s^{-1}) resulted in a rapid quenching of the NADPH-induced fluorescence to the initial (light-induced) F_m level the HA/DCMU treated sample, which then recovered with kinetics similar to that for the initial NADPH-induced rise (Fig. 1(a)). For comparison purposes, normalised F_{npr} data from Fig. 1(a) are presented in Fig. 1(b). The initial slope of the HA/DCMU-treated sample is 85% of that of the untreated control. A very small degree of sigmoidicity is apparent in the untreated sample, which disappears upon addition of HA/DCMU, presumably reflecting the removal of a minor secondary component of the reaction on HA/DCMU treatment.

It is unlikely that hydroxylamine itself acts as a simple Stern–Vollmer quencher under the conditions employed here as the value of F_m obtained by saturating pulse was unchanged in the presence of 1 mM HA compared to the untreated control (Fig. 1(a)).

To control for the effect of irreversible inactivation of the PSII oxygen evolving complex via manganese loss due to hydroxylamine treatment [42,43], HA was added to the lysed chloroplasts in situ immediately prior to the start of the chlorophyll fluorescence data collection. Increasing the HA concentration to 5-, 10- and 20 mM respectively in the presence of 10 μM DCMU resulted in the progressive diminishment of the F_{npr} such that the amplitude of the rise observed with 20 mM HA was 35% of that observed with 1 mM HA (Fig. S2). F_v/F_m in osmotically ruptured chloroplasts subject to a 60 second wash in 1 mM HA was observed to be 0.68 ± 0.02 (n = 3), compared to 0.77 ± 0.01 in the untreated sample, which likely reflects loss of OEC function in a small proportion of centres even under conditions of rapid initiation of the F_{npr} measurements.

The effect of oxygen on the F_{npr} signal in the presence of HA and DCMU is presented in Fig. 1(c). Oxygen may act as an electron sink for the PQ pool via plastoquinol oxidase (PTOX) activity or undergo one-electron reduction from reduced Fd, generating superoxide [44,45]. The kinetics of the rise are similar in both anaerobic- and aerobic conditions, although the amplitude of the F_{npr} signal is approximately 10% larger under anaerobic conditions.

3.1.2. Cytochrome b559

The biological role of cytochrome *b*559, a heterodimeric haemoprotein of apparently variable redox potential within PSII, remains enigmatic [46]. To investigate for the participation of this redox protein in dark, NADPH-dependent processes within PSII, decay-associated visible absorption spectra were constructed from kinetic data obtained via absorbance measurements at 540-, 550-, 560-, 566- and 573 nm upon addition of 100 μM NADPH to osmotically ruptured spinach chloroplasts in osmotic lysis buffer in the presence of 5 μM Fd.

No redox changes attributable to cytochrome *b*559 were observed in the decay-associated spectra generated from these measurements. Gaussian fitting of decay-associated spectral data revealed a single component with a peak at 555 nm, which was attributed to cytochrome *f* reduction (Fig. S3).

3.1.3. DPI and antimycin A sensitivity

The requirement for exogenous Fd in the NADPH-associated chlorophyll fluorescence rise suggests the participation of ferredoxin: NADP + oxidoreductase (FNR). This was tested by the addition of 10 μM diphenyleneiodonium chloride (DPI), a general flavoenzyme irreversible inhibitor [47], which abolished the F_{npr} signal (Fig. 2). The effect of DPI on the NADPH-dependent Fd:cytochrome *c* reductase activity of purified spinach FNR was then investigated; enzymatic activity was completely inhibited in the presence of 10 μM DPI (Fig. 3).

The effect of antimycin A on the kinetics of the NADPH-associated fluorescence rise in osmotically ruptured chloroplasts is presented in Fig. 4. 'Fractional activity' for inhibition was calculated by measuring the rate of the fluorescence rise for a 30 s interval after NADPH addition using a linear fit. In agreement with the observation of others [24,29], the NADPH-associated fluorescence rise was antimycin A-sensitive,

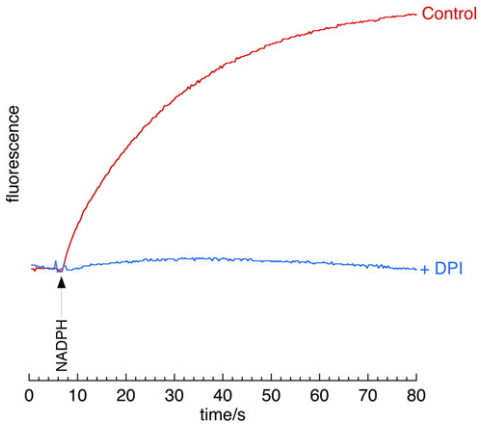

Fig. 2. The effect of diphenyleneiodonium chloride (DPI) on F_{npr}. The chlorophyll fluorescence rise in osmotically ruptured spinach chloroplasts (20 μg Chl ml^{-1}) was monitored in the absence (blue) and presence (red) of 10 μM DPI. Addition of 100 μM NADPH is indicated by the arrow. The assay buffer consisted of 10 mM HEPES (pH 7.6), 10 mM $MgCl_2$, 1 mM HA, 10 μM DCMU, 5 μM Fd. The initial saturating pulse (SP) prior to the addition of 100 μM NADPH is not shown.

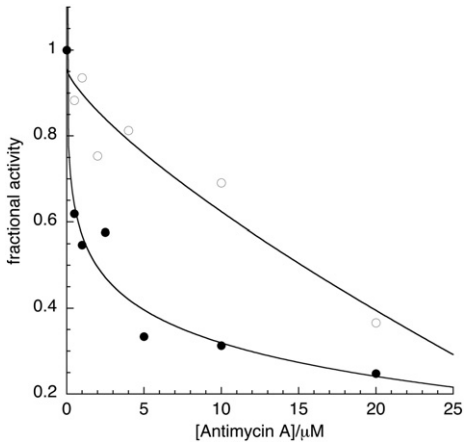

Fig. 4. The effect of antimycin A (AA) on F_{npr} in osmotically ruptured spinach chloroplasts. The effect of AA on F_{npr} was measured in the presence (○) and absence (□●) of 1 mM HA, 10 mM DCMU. Fractional activity for inhibition was calculated from the gradient of the linear portion of fluorescence rise following normalisation to the maximum extent of the rise. Osmotically ruptured chloroplasts were incubated with antimycin A for 1 min prior to the addition of 100 μM NADPH. Assay conditions are otherwise identical to those presented in Fig. 1(a).

with an effective IC_{50} for antimycin A of 2 μM. The IC_{50} value increased to 10 μM in the presence of 1 mM HA and 10 μM DCMU. Using purified spinach FNR, no inhibition of NADPH-dependent Fd:cytochrome *c* reductase activity was observed in the presence of 10 μM antimycin A (Fig. 3), indicating that its site of action is not in FNR.

3.1.4. The redox properties of the F_{npr} component

The F_{npr} signal in the presence of NADPH was quenched by the addition of an equimolar amount of $NADP^+$, indicating that the F_{npr} signal is reversible and that NADPH must be predominantly reduced to initiate it. This indicates that the F_{npr} quencher is associated with a strongly reducing redox carrier. Titration of the NADPH:$NADP^+$ molar ratio (at a constant NADPH concentration of 100 μM to control for mass action effects) in osmotic lysis buffer supplemented with 5 μM Fd indicated an apparent midpoint potential for the F_{npr} component of <−340 mV at pH 7.6 (Fig. 5) under aerobic- and anaerobic conditions. It is important to note that the observed midpoint potential represents a minimum value as the maximum extent of the F_{npr} rise is not known (i.e. the redox titration is incomplete). The midpoint potential of this quenching response was unaltered by the presence of 10 μM DCMU and 1 mM HA.

3.1.5. Room temperature chlorophyll fluorescence emission spectroscopy

To investigate the possibility that F_{npr} originated from photosystem I or associated antenna, room temperature chlorophyll fluorescence emission difference spectra were obtained upon the addition of 100 μM NADPH to osmotically ruptured chloroplasts (20 μg Chl ml^{-1}) in osmotic lysis buffer supplemented with 5 μM Fd. The experiment was then repeated in the presence of 10 μM DCMU and 1 mM hydroxylamine (Fig. 6(a–b)). As an additional control, difference spectra were obtained with osmotically ruptured chloroplasts upon addition of 10 μM DCMU in the absence of NADPH (Fig. 6(a–b)). Photosystem I-attributable fluorescence changes would be expected to occur in the

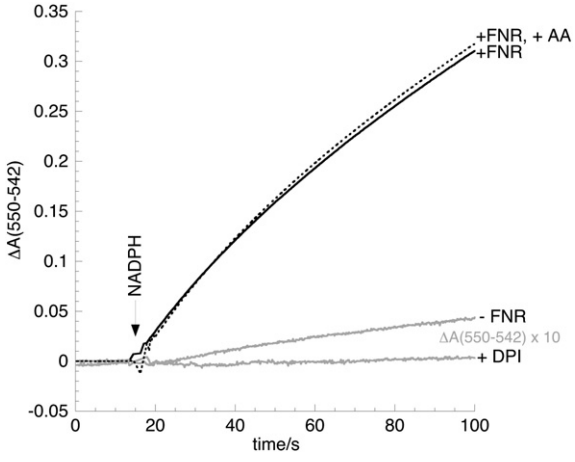

Fig. 3. The effect of inhibitors on spinach FNR activity. FNR turnover was monitored spectrophotometrically as NADPH-linked Fd:cytochrome c reductase activity at 550 *minus* 542 nm. All experiments were performed in an assay buffer consisting of 50 mM potassium phosphate (pH 7.5), 2 mM EDTA supplemented with 5 mM Fd. The FNR concentration was approximately 1.5 μg ml^{-1}. The reaction was initiated by the addition of 100 μM NADPH. The kinetic data represented by the broken black line were obtained in the presence of 10 μM antimycin A (AA). The control experiment (performed in the absence of AA) is shown in solid black. The broken grey line (+DPI) shows the effect of 10 μM DPI on FNR activity. The solid grey line (−FNR) shows the rate of non-enzymatic cytochrome c reduction in the presence of NADPH and Fd. Please note the 10-fold increase in absorbance scale in the lower two traces compared to the upper.

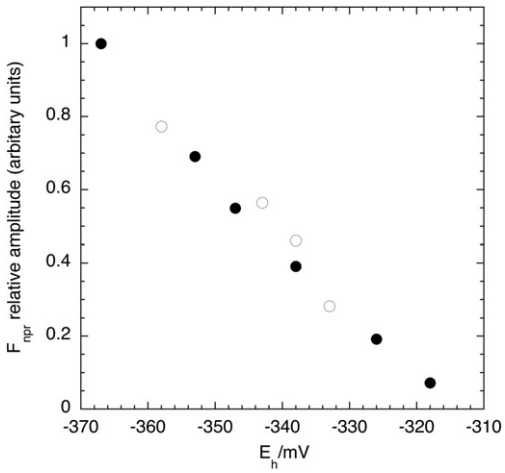

Fig. 5. Redox titration of F_{npr} in osmotically ruptured spinach chloroplasts. The redox titration of the F_{npr} signal was performed at 21 °C by varying the ratio of [$NADP^+$] to [NADPH] at a constant NADPH concentration of 100 μM. $NADP^+$ was added to the assay buffer (10 mM HEPES, 10 mM $MgCl_2$, 5 μM Fd, pH 7.6) prior to the addition of NADPH. Chlorophyll concentration was 20 μg Chl ml^{-1}. The amplitude of the F_{npr} was measured 2 min after NADPH addition. Filled- and open circles indicate data obtained under aerobic and anaerobic conditions respectively. E_h was calculated from the Nernst equation, assuming an $E_{m,7.6}$ for NADPH of −338 mV. The $E_{m,7.6}$ of −345 mV for the F_{npr} obtained from this plot represents a minimum value, as the maximum extent of the fluorescence rise is not known.

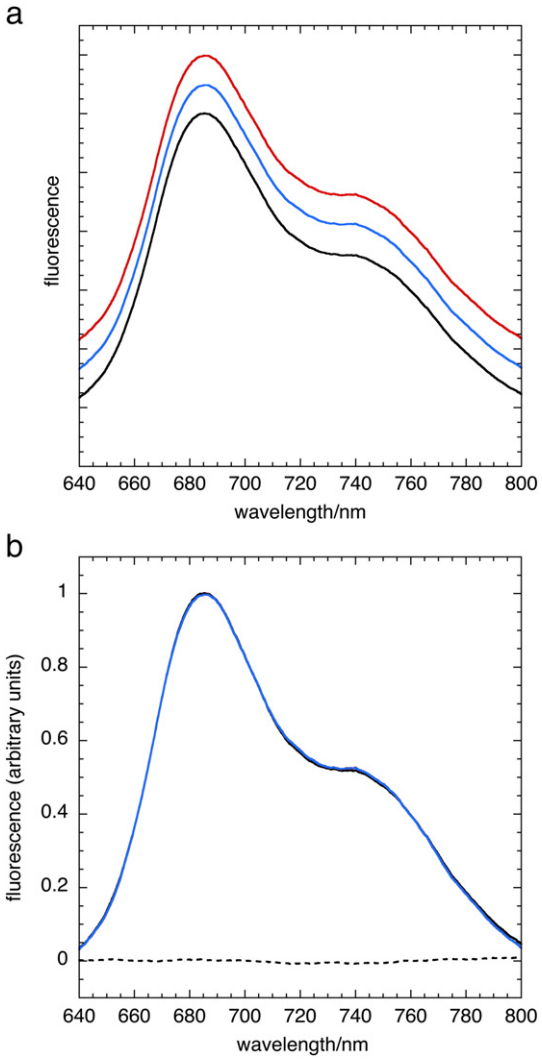

Fig. 6. Room temperature chlorophyll fluorescence emission difference spectra. Panel (a) room temperature chlorophyll fluorescence emission difference spectra obtained 2 min after the addition of 100 μM NADPH to osmotically ruptured spinach chloroplasts (20 μg Chl ml^{-1}) in the presence- (red spectrum) and absence (black spectrum) of 1 mM HA, 10 μM DCMU respectively. The blue spectrum was obtained upon addition of 10 μM DCMU to osmotically ruptured chloroplasts, in the absence of NADPH. All differences were obtained in an assay buffer consisting of 10 μM HEPES (pH 7.6), 10 mM $MgCl_2$, 5 μM Fd. Spectra were normalised to the emission peak at 684 nm, and have been offset for clarity in this figure. Panel (b): overlay of spectra from panel (a). The black dotted line shows the double difference chlorophyll fluorescence emission spectrum obtained from subtracting the blue spectrum (NADPH, HA, DCMU-containing sample) from the black spectrum (NADPH only).

long wavelength (740 nm) region of the spectra, but no significant differences were observed between the sets of difference spectra under the conditions employed. As such, there was no evidence for changes in PSI-associated variable fluorescence on NADPH addition.

3.1.6. 77 K fluorescence spectra

The effect of NADPH on the chlorophyll fluorescence emission spectra at 77 K was then examined (Fig. 7). Spinach chloroplasts were diluted to 4.0 μg Chl ml^{-1} in osmotic lysis buffer (supplemented with 5 μM Fd) and fluorescence emission spectra of samples were recorded at 77 K before- and 2 min after the addition of 100 μM NADPH. Spectra were normalised to the emission peak at 694 nm. Only minor changes were observed in the 77 K fluorescence emission spectra on NADPH addition, namely a 4% decrease in the intensity of the fluorescence emission peak at 735 nm, a 1 nm hypsochromic (blue) shift and 2% increase in intensity of the peak at 694 nm, and a slight broadening and quenching (2%) of the peak at 685 nm. Addition of 10 μM DCMU

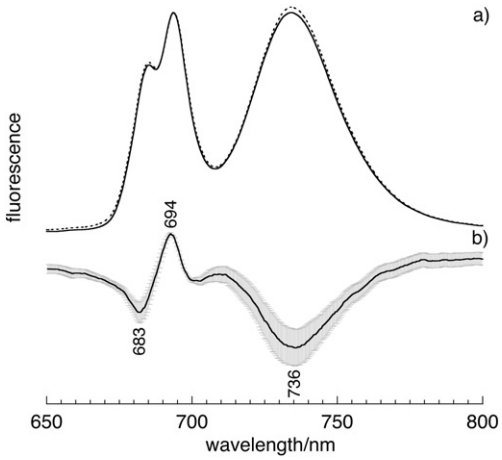

Fig. 7. (a) The effect of NADPH on the 77 K chlorophyll fluorescence emission spectra of ruptured spinach chloroplasts. Samples consisted of spinach chloroplasts (4 μg Chl ml^{-1}) in 10 mM HEPES (pH 7.6), 10 mM MgCl2, 5 μM Fd prior to- and 2 min after the addition of 100 μM NADPH (broken- and solid lines respectively). Four absolute spectra were averaged per sample before- and after NADPH addition, with four discrete samples used to generate the data shown above. Spectra were normalised to the emission peak at 694 nm. (b) 77 K chlorophyll fluorescence emission difference spectrum obtained on NADPH addition (+NADPH *minus* no addition). The scale of the ordinate is multiplied 10× compared to that in panel (a). Peaks are labelled. Error bars correspond to the SD (n = 16).

resulted in a 2 nm hypsochromic shift of the 685- and 694 nm peaks. As a consequence of the interference from this DCMU-induced hypsochromic effect, 77 K spectra were not obtained in the presence of hydroxylamine and DCMU.

3.2. The role of the PQ pool in F_{npr}

3.2.1. Fluorescence induction analysis of PQ pool reduction

The complementary area between a chlorophyll fluorescence induction curve and F_m obtained by a saturating pulse provides information concerning the degree of reduction of the acceptor (PQ) pool [48–50]. The effect of NADPH addition on the redox status of the PQ pool in the dark was investigated by this method. Fig. 8 displays the fluorescence induction curves obtained from osmotically ruptured spinach chloroplasts using a 400 ms saturating light pulse (620 nm) before- and 2 min after addition of 100 μM NADPH (in the presence of 5 μM Fd). The area bounded by the fluorescence induction curve and F_m was 48%

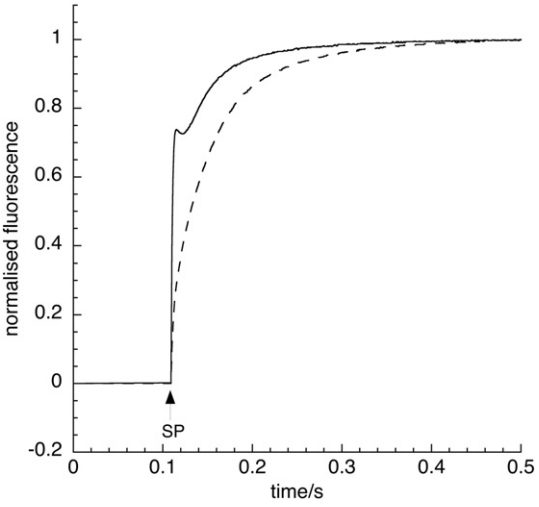

Fig. 8. Normalised fluorescence induction curves obtained before (broken line) and 2 min after (solid line) the addition of 100 μM NADPH to osmotically ruptured spinach chloroplasts (20 μg Chl ml^{-1}). The assay buffer consisted of 10 mM HEPES (pH 7.6), 10 mM $MgCl_2$, 5 mM Fd. The application of the saturating pulse is indicated by 'SP'.

smaller after the addition of NADPH, indicative of a partial reduction of the PQ pool in the dark by the addition of NADPH + Fd, but with kinetics approximately 1.5-fold slower than the reduction of the F_{npr} quencher, and comparable to the inter-system chain reduction kinetics discussed below.

It is important to note that chlorophyll fluorescence yield is inversely (rather than linearly) related to the rate constant for quenchers [51,52]. This means that the weak F_{npr} signal probably underestimates to some extent the rate of NADPH-induced change in concentration. Thus the F_{npr} quencher is eliminated more rapidly than bulk PQ is reduced. Also, despite its relatively high redox midpoint potential, the PQ reduction was only partial at the end of the experiment, whereas the more reducing F_{npr} component was saturated. These results indicate that F_{npr} and PQ do not reach redox equilibrium over the time scale of minutes.

3.2.2. Effect of tridecylstigmatellin

Oxidised quinones can act as quenchers of chlorophyll fluorescence through direct interactions with chlorophylls [53]. The native PQ pool has been observed to act as an effective quencher in thylakoid preparations [54], although vacuum infiltration with DCMU is reported to be necessary to induce PQ-mediated quenching in leaves [55]. To test if the fluorescence quencher associated with F_{npr} could be attributed to PQ quenching, we assessed the effects of tridecylstigmatellin (TDS), a tightly-binding, competitive inhibitor of plastoquinol oxidation within the cytochrome b_6f complex [56,57] on the redox and light dependence of F_{npr}. Osmotically ruptured chloroplasts (20 μg Chl/ml) were incubated on ice in osmotic lysis buffer with an excess of TDS (1 μM) for 5 min prior to the addition of DCMU, HA, Fd and NADPH. The sensitivity of the cytochrome b_6f complex to stigmatellin under these conditions was confirmed by monitoring the retardation of the rate of P_{700}^+ re-reduction (ΔA700 nm) following far-red excitation upon addition of 1 μM TDS in DCMU-inhibited chloroplasts in the presence of 100 μM NADPH and 5 μM Fd (Fig. S4). However, TDS had no effect on the kinetics of the NADPH-induced fluorescence rise, nor the FR-induced quenching and subsequent recovery (Fig. 9), indicating that the F_{npr} signal was independent of the activity of the cytochrome b_6f complex and by extension, the redox state of the bulk PQ pool.

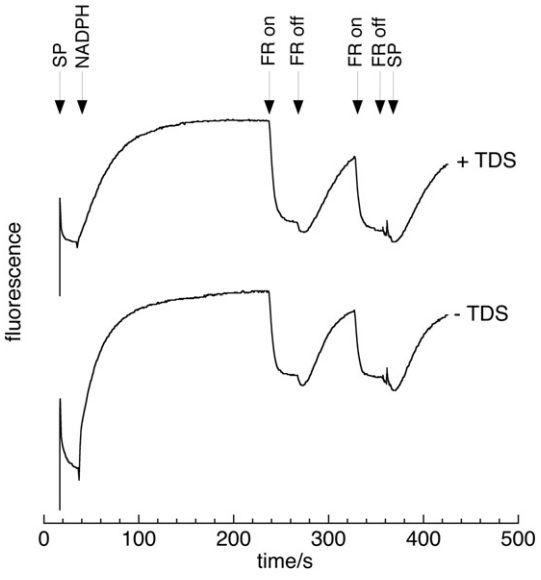

Fig. 9. The effect of tridecylstigmatellin (TDS) on F_{npr} in osmotically ruptured spinach chloroplasts. Assay conditions in the presence (upper trace) and absence (lower trace) of 1 μM TDS are as in Fig. 1. All experiments were performed in the presence of 10 μM DCMU, 1 mM HA. The osmotically ruptured chloroplasts were incubated with TDS for 5 min before the addition of 100 μM NADPH. The saturating pulse (620 nm) is indicated by 'SP'. The period of illumination by far-red light is indicated by 'FR on' and 'FR off'.

3.2.3. Comparison of the F_{npr} and intersystem chain reduction kinetics

The reduction status of the thylakoid intersystem chain (i.e. the size of the pool of reduced donors to PSI) in the presence of NADPH, Fd and DCMU can also be assessed by monitoring the kinetics of P_{700} oxidation by far-red illumination [20,58], varying the duration of the dark interval between periods of PSI excitation. Turnover numbers in the order of 50–200 s^{-1} have been reported for the cytochrome b_6f complex in thylakoid preparations, and so this enzymatic activity is unlikely to be limiting for P_{700}^+ re-reduction under the conditions employed here [59]. The oxidation kinetics of the intersystem chain by P_{700}^+ during far-red actinic illumination (Fig. 10(a–c)) were compared with the F_{npr} kinetic data from Fig. 1(a). Reduction of the intersystem carriers in the presence of 100 μM NADPH and 5 μM Fd (with 10 μM DCMU and 1 mM HA) was approximately 1.5-fold slower than that observed for F_{npr} under equivalent conditions, with respective half-times of 35 and 20 s, despite the fact that the intersystem pool carriers have a much higher redox potential than the F_{npr} component, confirming a lack of redox equilibrium between these components over the minutes time scale.

4. Discussion

We present a systematic investigation of the F_{npr} signal in vitro, to test its functional and physiological implications. Our results are clearly at odds with the accepted (and expected) model in which F_{npr} reflects the reduction of PQ by the CEF-related plastoquinone reductases. Multiple lines of evidence show that the major F_{npr} component in isolated thylakoids does not rapidly equilibrate with the redox state of the PQ pool, and therefore does not directly reflect the CEF-associated PQ reductase activity. Notably, F_{npr} is unaffected by treatments that should alter the redox state of the PQ pool, including the addition of TDS together with illumination by far-red or red light, or the addition of DCMU and HA (Figs. 1 and 9) which should prevent PQ from binding to the Q_B site and inhibit the oxidation of photoreduced Q_A. Also, the kinetics of the fluorescence rise are faster than those inferred for the (non-LEF) in vitro reduction of the thylakoid intersystem chain obtained by measuring the rate of P_{700} oxidation in the presence of NADPH, Fd, DCMU and hydroxylamine. In addition, the redox potential of the F_{npr} component estimated by redox titration with $NADP^+$/NADPH (Fig. 5) was approximately −340 mV (a minimum value), far too negative to be effectively reduced by bulk PQ.

The sensitivity of the F_{npr} signal to assay conditions (Fig. 1(a)) and inhibitors (Figs. 2 and 4) reported here is in agreement with previous work [15,22] on the requirement for F_{npr} for Fd that is reduced through the activity of FNR ([24,25], see Figs. 2 and 3). Taken together, these results place the F_{npr} redox component within PSII or associated complexes, most likely a low potential form of Q_A that is directly reducible by Fd (represented in model form in Fig. 11). Because F_{npr} does not appear to rapidly reduce the PQ pool, this putative Q_A population should be associated with PSII centres lacking functional, or otherwise modified, Q_B sites.

We also confirm the antimycin A sensitivity of the F_{npr} signal [15,24], which has been assumed to be a direct consequence of PQR inhibition [12,60]. However, multiple effects have been ascribed to the interaction of antimycin A and the thylakoid electron transfer chain, and the mechanism of action of this inhibitor on photosynthetic processes is poorly understood. Aside from acting as a PQR-dependent CEF inhibitor, antimycin A has been proposed to diminish qE through either LHCII disaggregation or protonophoric activity [61–63] to act as an ADRY reagent [64] and to inhibit cytochrome *b*559 photoredox chemistry [65,66]. Additionally, relatively high (micromolar) concentrations of antimycin A are required for inhibitory effect on photosynthetic processes [12,13]. It thus seems likely that antimycin A has multiple (or even global) effects on photosynthesis, and thus ascribing functional significance to any one process may be misleading.

Intriguingly, we note that the apparent IC_{50} for antimycin A activity on the NADPH-associated fluorescence rise increases approximately

five-fold higher in the presence of DCMU and hydroxylamine (Fig. 4), most likely reflecting changes the influence of conformational or redox changes in PSII on F_{npr}. We hypothesise that antimycin A inhibits (either directly or through secondary effects on supercomplex organisation) the interaction between reduced Fd and its low potential acceptor within PSII, in a comparatively weak competitive- or non-competitive manner. This proposed interaction between antimycin A and PSII is compatible with the observations of the apparent chaotrophic effect of antimycin A on photosystem organisation by Oxborough and Horton [61], or the ADRY phenomenon noted by Yerkes and Crofts [64].

4.1. Relationship to the question of Q_A redox potential

There is a large degree of variation in reported literature values for the midpoint potential of Q_A. Early work measuring chlorophyll fluorescence yield changes as a function of redox potential reported two midpoint potentials at −270 and −35 mV [67–69]. Additional studies, mostly with eukaryotic material, confirmed the presence of a quencher with a midpoint potential of approximately -275 ± 50 mV, with a second quenching species with a midpoint potential of around 0 ± 100 mV (reviewed by [68]). These data were obtained under a variety of conditions from a number of different species, in the presence- and absence of inhibitory treatments and exogenous redox mediators (which may act as chlorophyll fluorescence quenchers, or affect the E_m of Q_A via Q_B antagonism [70,68]), hindering direct comparison. More recent studies with PSII-enriched samples report midpoint potentials of approximately −160 mV and −80 mV for spinach Q_A[68,69]. The presence of a low potential variant of Q_A, and associated PSII structural heterogeneity, was also inferred from redox titration of the photoinduced EPR spectrum of pheophytin in spinach chloroplast preparations [71].

It is also clear that the midpoint potential of Q_A is sensitive to the nature of the occupant within Q_B site and the functional status of the oxygen evolving complex [72–75] as well as local structural (electrostatic and hydrogen-bonding) perturbation [76,77]. This sensitivity of Q_A redox potential may extend to the physiologically relevant phosphorylation of D1 protein involved in post-photoinhibition repair ([78] and references therein). In turn, D1 phosphorylation may, in part, contribute to the phenomenon of 'Q_B-non-reducing' (or 'inactive') centres, which are estimated to form 5–10% of the PSII population in non-stressed plant material [79,80]. To our knowledge, the redox potential of Q_A has not been measured in phosphorylated PSII, although it seems likely that it would be affected by a change in the local electrostatic environment.

4.2. Q_B-bypassing electron transfer between Q_A and stromal redox partners

Inspection of the atomic structure of *Thermosynechococcus vulcanas* PSII [81] reveals a separation of 6.5 Å from the plastoquinone headgroup of Q_A to the stromally-exposed DE loop of D1, the proposed target site for DegP2 (and FtsH) protease activity [82,83]. We note that on distance dependency constraints the proximity of Q_A to the stromal phase would allow a Q_B-bypassing electron transfer shunt on the millisecond timescale if the formation of the encounter complex is energetically favourable [84]. Q_B bypass reactions to soluble acceptors are not unprecedented; the magnesium-dependent oxidation of Q_A^- in DCMU-inhibited spinach chloroplasts by ferricyanide has a second order rate constant of 30 M^{-1} s^{-1} at pH 7.6 [85,86]. DCMU-insensitive photoreduction of exogenous cytochrome *c*, with concomitant oxygen evolution, has been observed in genetically modified *Synechocystis PCC* 6803 PSII preparations containing the D1-Lys238Glu mutation [87]. This residue is located at the edge of a cluster of positive

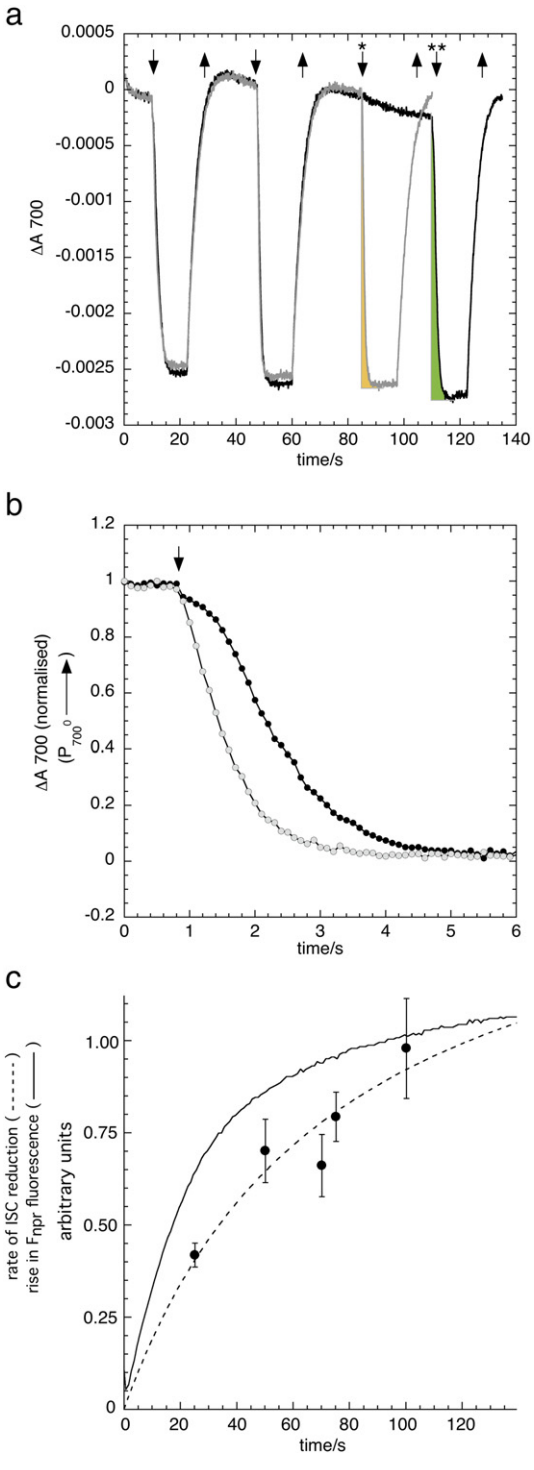

Fig. 10. (a) P_{700} oxidation kinetics in osmotically ruptured spinach chloroplasts in the presence of DCMU, hydroxylamine and NADPH. The downward- and upward arrows indicate the application and removal of far-red actinic illumination. P_{700} oxidation was measured at 700 nm. Two representative kinetic traces are shown with varying duration of the third dark period (grey trace, $t_{dark} = 25$ s, indicated by the single asterisk; black trace, $t_{dark} = 50$s, indicated by the double asterisk). The assay buffer consisted of 10 mM HEPES (pH 7.6), 10 mM $MgCl_2$, 5 μM Fd, 1 mM HA, 10 μM DCMU. Chlorophyll concentration was 40 μg Chl ml^{-1}. The yellow and green shaded areas are indicators of the size of the pool of reduced electron donors to P_{700}^+. The size of these shaded areas was measured by integration (Kaleidagraph, Synergy Software Inc.). (b) Expansion and overlay of the P_{700} oxidation kinetics for the third dark period from panel (a). Grey circles indicate ΔA 700 for $t_{dark} = 25$ s, black circles correspond to $t_{dark} = 50$s. The downward arrow indicates the application of far-red illumination. (c) Comparison of the F_{npr} kinetics (solid line) and the size of the pool of reduced ISC donors to P_{700}^+ as a function of time (broken line). The F_{npr} kinetics measurements were performed with the same chloroplast preparation as that used for (and in concert with) the ΔA 700 measurements. The error bars indicate the standard deviation ($n = 3$).

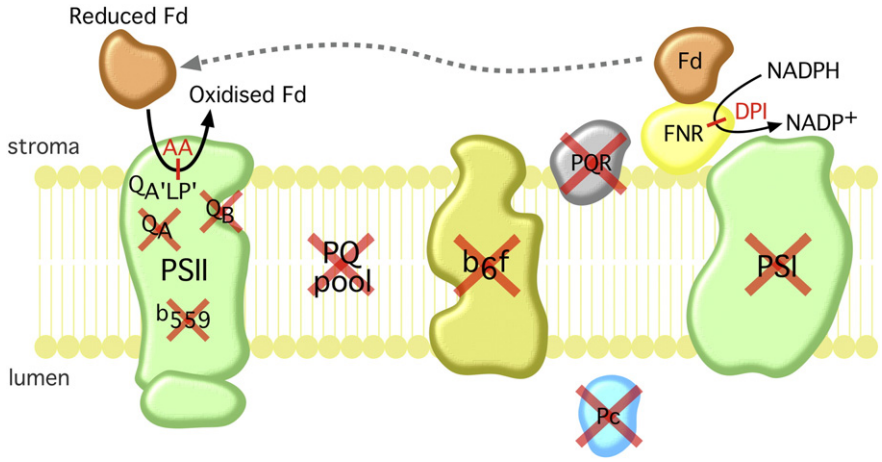

Fig. 11. Working model for the F_{npr} phenomenon within the thylakoid membrane. NADPH-reduced Fd reduces a low potential variant of Q_A ($Q_{A'LP'}$) within PSII. Only a small population of photocentres are reducible in this manner. Redox components not associated with the F_{npr} are scored out in red. Electron transfer stoichiometry is not shown. Sites of inhibition by DPI and (putatively) antimycin A (AA) are indicated. Cytochrome *b*559, plastoquinone, plastocyanin (ferredoxin):plastoquinone reductase and ferredoxin:$NADP^+$ reductase are abbreviated as *b*559, PQ, Pc, PQR and FNR respectively.

electrostatic potential at the surface of D1 approximately equidistant between Q_A and Q_B, with a closest approach to Q_A of 15 Å. This modification was observed to be photoprotective in vitro in the presence of oxidised cytochrome *c*. Similarly, in a recent study by Zhang et al. [88], a Q_B-bypassing electron transfer reaction in native cyanobacterial PSII to a soluble flavoprotein complex is posited as a photoprotective mechanism.

This probable location of the F_{npr} component is compatible with PSII centres participating in the photorepair cycle [89]. For steric reasons, access of Fd to Q_A would be restricted to non-appressed (stromal) regions of the thylakoid membrane, probably on the granal margins. PSII 'β'centres, which are considered to be excitonically disconnected from other photosystems, are also proposed to be located within the stromal lamellae [90]. As a whole, only a minor fraction of the total PSII population would be accessible to Fd, as observed. We note that the NADPH-associated fluorescence rise is magnesium-dependent [24]. Whilst thylakoids prepared in the absence of exogenous Mg^{2+} are expected to be unstacked [91] and the PSII likely accessible to Fd, the strongly anionic nature of Fd (pI = 3.9, spinach Fd) may necessitate electrostatic screening by cations for formation of the encounter complex for photosystem interaction.

4.3. On the phenomenon of F_{npr} quenching during red or far-red illumination

Application of far-red light to Fd + NADPH-treated thylakoids leads to a reversible quenching of fluorescence (Fig. 1(a)). The obvious interpretation of this effect is that activation of PSI photochemistry results in the oxidation of plastoquinol reduced by NADPH. However, we present three lines of evidence that this interpretation is incorrect. First, the effect is insensitive to saturating (micromolar) concentrations of tridecylstigmatellin, a potent inhibitor of plastoquinol oxidation by the cytochrome b_6f complex. Second, the quenching is unaffected by the presence of hydroxylamine and DCMU, inhibiting Q_A^- oxidation. Finally, the effect is similar with red or far-red illumination and thus cannot be attributed to preferential excitation of PSI. We conclude that the quencher is not associated with photosystem I-mediated photooxidation of the PQ pool.

Within PSII, P_{680}^+ itself and the photooxidizable carotenoid (Car) and Chl_{ZD1} components of the 'secondary' electron transport chain can act as quenchers of chlorophyll fluorescence. This chain is proposed to reduce P_{680}^+ via cytochrome *b*559 when the donor side is inhibited, using electrons from Q_B or the PQ pool, such as may occur following damage to the OEC [46,92]. P_{680}^+ is a highly oxidising species ($E_{m,7} \geq +1.2$ V) with a sub-millisecond lifetime in the presence of millimolar hydroxylamine (which serves as a Tyr_z reductant) [93,94], and so is unlikely to be a contributory factor to the initial F_{npr} rise kinetics in Fig. 1(a) (lower trace). We cannot exclude the participation of P_{680}^+ in the F_{npr} quenching response induced by red- or far-red illumination as this species is a very efficient oxidant of Q_A^- [93]; the rate constant for P_{680}^+/Q_A^- recombination has been reported to be 6000 s^{-1} in manganese-depleted spinach thylakoids [95]. Recombination between (light-induced) Car^+/Chl_{ZD1}^+ and Q_A^- is likely to proceed much more slowly due to distance constraints (c. 40 Å separation) [96].

These fluorescence quenching results are at first sight similar to those described by Klimov et al. [97] who demonstrated that chlorophyll fluorescence was quenched by photoaccumulation of reduced pheophytin in pea subchloroplast particles in the presence of reductant. However, the red/far-red quenching phenomenon observed in the current study was unaffected by high concentrations (>10 mM) of HA (Fig. S2), conditions under which the oxygen-evolving complex is predicted to be depleted of manganese. Alteration of the PSII donor side in this manner would therefore be expected to affect the thermodynamics [98] and kinetics [99] of the system and subsequent quenching kinetics observed during red/far-red illumination. We thus conclude that the quenching is not related to pheophytin reduction in the bulk of PSII centres. On the other hand, the data presented above shows that the F_{npr} signal likely originates in a subpopulation of PSII centres with inactive Q_B sites, and it is likely that they also possess modified oxygen evolving complexes. We therefore suggest that the red/far-red quenching is related to the accumulation of yet unidentified quenching states in these special centres.

4.4. On the F_{npr} signal as an assay for CEF

There is strong evidence that the F_{npr} signal as observed as the post-illumination fluorescence rise in vivo is associated with the activity of the NDH complex and thus with the CEF or chlororespiration [10,26,27]. However, only a small fraction of the signal seen in vitro can be attributed to NDH activity, specifically the small residual signal in the *pgr5* mutant that is sensitive to the expression of NDH [26,29]. The loss of this signal, and the sluggishness of the rate of PQ pool reduction (Fig. 10(c)) (see also [22–24]), compared to ~10-fold higher rates of CEF estimated to occur under some conditions in vivo [18,19,31], are consistent with a loss in NDH-related PQ reductase activity upon isolation of thylakoids. This phenomenon is likely to be of physiological importance, representing either loss of an enzymatic component or the action of a CEF regulatory system (see also [32]).

The F_{npr} signal seen in isolated thylakoids has been attributed to the activity of the PGR5-related CEF [15,29]. The conclusion (above) that the in vitro F_{npr} signal is not associated with the reduction of the bulk PQ pool and thus unlikely to be directly involved in CEF, complicates the interpretation of some past results. The major photosynthetic phenotype of *pgr5* is a general loss of light-driven proton gradient and the decrease in amplitude of the F_{npr} signal in *pgr5* was taken as critical support for the direct involvement of PGR5 in the "main" pathway for CEF [15,29]. However, it is clear that CEF can proceed in the absence of PGR5 [19,21,100] and an alternative interpretation has been proposed wherein the loss of proton gradient in this mutant results not from changes in CEF but in the loss of control of regulation of the chloroplast ATP synthase [18,21]. The *pgr5* mutant appears pleiotropic with effects on several photosynthetic processes as well as thylakoid ultrastructure [101]. It is also clear that the thylakoid electron transfer chain in *pgr5* is prone to over-reduction with subsequent effects on photoprotection and PSI photodamage [18,19,21,32]. It is thus unclear whether the apparent inhibition of the F_{npr} component is a cause or an effect of the *pgr5* mutation. Moreover, we conclude that, by itself, the F_{npr} signal as observed in vitro in thylakoids or osmotically ruptured chloroplast preparations on addition of Fd and NADPH should not be considered a useful reporter for CEF activity and likely results from the direct reduction of a subpopulation of Q_A by ferredoxin in an antimycin A-sensitive process.

Supplementary data to this article can be found online at http://dx.doi.org/10.1016/j.bbabio.2014.09.005.

Acknowledgements

This work was supported by the grant DE-FG02-11ER16220 (to D.M.K.) from the Division of Chemical Sciences, Geosciences, and Biosciences, Office of Basic Energy Sciences of the US Department of Energy. We would like to thank Prof. Charles Yocum (University of Michigan), Prof. William Rutherford (Imperial College), Prof. William Cramer (Purdue University), Dr. Derek Bendall (University of Cambridge) and Deserah Strand (Michigan State University) for useful discussions during the preparation of this manuscript.

References

[1] P. Mitchell, Protonmotive Q-cycle — general formulation, FEBS Lett. 59 (1975) 137–139.
[2] D.R. Ort, C.F. Yocum, Electron transfer and energy transduction in photosynthesis: an overview, in: D.R. Ort, C. Yocum, I. Heichel (Eds.), Oxygenic Photosynthesis: The Light Reactions, Springer, Netherlands, 1996, pp. 1–9.
[3] J.F. Allen, Cyclic, pseudocyclic and noncyclic photophosphorylation: new links in the chain, Trends Plant Sci. 8 (2003) 15–19.
[4] P. Horton, A.V. Ruban, R.G. Walters, Regulation of light harvesting in green plants, Annu. Rev. Plant. Physiol. Plant. Mol. Biol. 47 (1996) 655–684.
[5] J.A. Cruz, T.J. Avenson, A. Kanazawa, K. Takizawa, G.E. Edwards, D.M. Kramer, Plasticity in light reactions of photosynthesis for energy production and photoprotection, J. Exp. Bot. 56 (2005) 395–406.
[6] D.M. Kramer, T.J. Avenson, A. Kanazawa, J.A. Cruz, The relationship between photosynthetic electron transfer and its regulation, in: G. Papageorgiou, Govindjee (Eds.), Chlorophyll a Fluorescence: A Signature of Photosynthesis (Advances in Photosynthesis and Respiration), Springer, Dordrecht, 2004, pp. 251–278.
[7] T. Shikanai, Cyclic electron transport around photosystem I: genetic approaches, Annu. Rev. Plant Biol. 58 (2007) 199–217.
[8] G.N. Johnson, Physiology of PSI cyclic electron transport in higher plants, Biochim. Biophys. Acta 1807 (2011) 384–389.
[9] D.D. Strand, D.M. Kramer, Control of non-photochemical exciton quenching by the proton circuit of photosynthesis, in: B. Demmig-Adams, G. Garab, W.W. Adams, Govindjee (Eds.), Non-Photochemical Fluorescence Quenching and Energy Dissipation in Plants, Algae, and Cyanobacteria (Advances in Photosynthesis and Respiration), Springer, Dordrecht, 2014, (in press).
[10] P.A. Burrows, L.A. Sazanov, Z. Svab, P. Maliga, P.J. Nixon, Identification of a functional respiratory complex in chloroplasts through analysis of tobacco mutants containing disrupted plastid ndh genes, EMBO J. 17 (1998) 868–876.
[11] K. Ifuku, T. Endo, T. Shikanai, E.-M. Aro, Structure of the chloroplast NADH dehydrogenase-like complex: nomenclature for nuclear-encoded subunits, Plant Cell Physiol. 52 (2011) 1560–1568.
[12] D.A. Moss, D.S. Bendall, Cyclic electron transport in chloroplasts. The Q-cycle and the site of action of antimycin, Biochim. Biophys. Acta 767 (1984) 389–395.
[13] D.S. Bendall, R. Manasse, Cyclic photophosphorylation and electron-transport, Biochim. Biophys. Acta 1229 (1995) 23–38.
[14] T. Shikanai, Central role of cyclic electron transport around photosystem I in the regulation of photosynthesis, Curr. Opin. Biotechnol. 26 (2014) 25–30.
[15] Y. Munekage, M. Hojo, J. Meurer, T. Endo, M. Tasaka, T. Shikanai, PGR5 is involved in cyclic electron flow around photosystem I and is essential for photoprotection in *Arabidopsis*, Cell 110 (2002) 361–371.
[16] G. DalCorso, P. Pesaresi, S. Masiero, E. Aseeva, D. Schünemann, G. Finazzi, P. Joliot, R. Barbato, D. Leister, A complex containing PGRL1 and PGR5 is involved in the switch between linear and cyclic electron flow in *Arabidopsis*, Cell 132 (2008) 273–285.
[17] A.P. Hertle, T. Blunder, T. Wunder, P. Pesaresi, M. Pribil, U. Armbruster, D. Leister, PGRL1 is the elusive ferredoxin–plastoquinone reductase in photosynthetic cyclic electron flow, Mol. Cell 49 (2013) 511–523.
[18] T.J. Avenson, J.A. Cruz, A. Kanazawa, D.M. Kramer, Regulating the proton budget of higher plant photosynthesis, Proc. Natl. Acad. Sci. U. S. A. 102 (2005) 9709–9713.
[19] B. Nandha, G. Finazzi, P. Joliot, S. Hald, G.N. Johnson, The role of PGR5 in the redox poising of photosynthetic electron transport, Biochim. Biophys. Acta 1767 (2007) 1252–1259.
[20] P. Joliot, G.N. Johnson, Regulation of cyclic and linear electron flow in higher plants, Proc. Natl. Acad. Sci. U. S. A. 108 (2011) 13317–13322.
[21] M. Suorsa, S. Järvi, M. Grieco, M. Nurmi, M. Pietrzykowska, M. Rantala, S. Kangasjärvi, V. Paakkarinen, M. Tikkanen, S. Jansson, E.-M. Aro, Proton gradient regulation5 is essential for proper acclimation of *Arabidopsis* photosystem I to naturally and artificially fluctuating light conditions, Plant Cell 24 (2012) 2934–2948.
[22] J.D. Mills, D. Crowther, R.E. Slovacek, G. Hind, R.E. McCarty, Electron transport pathways in spinach chloroplasts. Reduction of the primary acceptor of photosystem II by reduced nicotinamide adenine dinucleotide phosphate in the dark, Biochim. Biophys. Acta 547 (1979) 127–137.
[23] Q.J. Groom, D.M. Kramer, A.R. Crofts, D.R. Ort, The non-photochemical reduction of plastoquinone in leaves, Photosynth. Res. 36 (1993) 205–215.
[24] T. Endo, H. Mi, T. Shikanai, K. Asada, Donation of electrons to plastoquinone by NAD(P)H dehydrogenase and by ferredoxin-quinone reductase in spinach [*Spinacia oleracea*] chloroplasts, Plant Cell Physiol. 38 (1997) 1272–1277.
[25] S. Corneille, L. Cournac, G. Guedeney, M. Havaux, G. Peltier, Reduction of the plastoquinone pool by exogenous NADH and NADPH in higher plant chloroplasts: characterization of a NAD(P)H-plastoquinone oxidoreductase activity, Biochim. Biophys. Acta 1363 (1998) 59–69.
[26] E. Gotoh, M. Matsumoto, K.I. Ogawa, Y. Kobayashi, M. Tsuyama, A qualitative analysis of the regulation of cyclic electron flow around photosystem I from the post-illumination chlorophyll fluorescence transient in *Arabidopsis*: a new platform for the in vivo investigation of the chloroplast redox state, Photosynth. Res. 103 (2010) 111–123.
[27] T. Shikanai, T. Endo, T. Hashimoto, Y. Yamada, K. Asada, A. Yokota, Directed disruption of the tobacco ndhB gene impairs cyclic electron flow around photosystem I, Proc. Natl. Acad. Sci. U. S. A. 95 (1998) 9705–9709.
[28] M. Hashimoto, T. Endo, G. Peltier, M. Tasaka, T. Shikanai, A nucleus-encoded factor, CRR2, is essential for the expression of chloroplast ndhB in *Arabidopsis*, Plant J. 36 (2003) 541–549.
[29] Y. Munekage, M. Hashimoto, C. Miyake, K.-I. Tomizawa, T. Endo, M. Tasaka, T. Shikanai, Cyclic electron flow around photosystem I is essential for photosynthesis, Nature 429 (2004) 579–582.
[30] L. Peng, Y. Fukao, M. Fujiwara, T. Takami, T. Shikanai, Efficient operation of NAD(P)H dehydrogenase requires supercomplex formation with photosystem I via minor LHCI in *Arabidopsis*, Plant Cell 21 (2009) 3623–3640.
[31] J. Alric, J. Lavergne, F. Rappaport, Redox and ATP control of photosynthetic cyclic electron flow in *Chlamydomonas reinhardtii* (I) aerobic conditions, Biochim. Biophys. Acta 1797 (2010) 44–51.
[32] D.M. Kramer, J.R. Evans, The importance of energy balance in improving photosynthetic productivity, Plant Physiol. 155 (2011) 70–78.
[33] M. Plesnicar, D.S. Bendall, The plastocyanin content of chloroplasts from some higher plants estimated by a sensitive enzymatic assay, Biochim. Biophys. Acta 216 (1970) 192–199.
[34] B.B. Buchanan, D.I. Arnon, Ferredoxins from photosynthetic bacteria, algae, and higher plants, Methods Enzymol. 23 (1971) 413–440.
[35] D. Seigneurin Berny, D. Salvi, J. Joyard, N. Rolland, Purification of intact chloroplasts from *Arabidopsis* and spinach leaves by isopycnic centrifugation, Curr. Protoc. Cell Biol. 3 (30) (2008) 3.30.1–3.30.14.
[36] W.P. Inskeep, P.R. Bloom, Extinction coefficients of chlorophyll a and b in N, N-dimethylformamide and 80% acetone, Plant Physiol. 77 (1985) 483–485.
[37] C.C. Hall, J. Cruz, M. Wood, R. Zegarac, D. DeMars, J. Carpenter, A. Kanazawa, D. Kramer, Photosynthetic measurements with the Idea Spec: an integrated diode emitter array spectrophotometer/fluorometer, Photosynthesis: Research for Food, Fuel and Future (15th International Conference on Photosynthesis), 2013, pp. 184–188.
[38] T. Yonetani, G.S. Ray, Studies on cytochrome oxidase. VI. Kinetics of the aerobic oxidation of ferrocytochrome c by cytochrome oxidase, J. Biol. Chem. 240 (1965) 3392–3398.
[39] D.F. Ghanotakis, G.T. Babcock, Hydroxylamine as an inhibitor between Z and P680 in photosystem II, FEBS Lett. 153 (1983) 231–234.
[40] W.F. Beck, G.W. Brudvig, Reactions of hydroxylamine with the electron-donor side of photosystem II, Biochemistry 26 (1987) 8285–8295.
[41] J. Nugent, I.P. Muhiuddin, M. Evans, Effect of hydroxylamine on photosystem II: reinvestigation of electron paramagnetic resonance characteristics reveals possible S state intermediates, Biochemistry 42 (2003) 5500–5507.

[42] P. Horton, E. Croze, The relationship between the activity of chloroplast photosystem II and the midpoint oxidation–reduction potential of cytochrome b-559, Biochim. Biophys. Acta 462 (1977) 86–101.
[43] R.R. Sharp, C.F. Yocum, Factors influencing hydroxylamine inactivation of photosynthetic water oxidation, Biochim. Biophys. Acta 635 (1981) 90–104.
[44] G. Peltier, L. Cournac, Chlororespiration, Annu. Rev. Plant Biol. 53 (2002) 523–550.
[45] K. Asada, Production and scavenging of reactive oxygen species in chloroplasts and their functions, Plant Physiol. 141 (2006) 391–396.
[46] P. Pospísil, Enzymatic function of cytochrome *b*559 in photosystem II, J. Photochem. Photobiol. B 104 (2011) 341–347.
[47] B.V. O'Donnell, D.G. Tew, O.T. Jones, P.J. England, Studies on the inhibitory mechanism of iodonium compounds with special reference to neutrophil NADPH oxidase, Biochem. J. 290 (1993) 41–49.
[48] N. Murata, M. Nishimura, A. Takamiya, Fluorescence of chlorophyll in photosynthetic systems II. Induction of fluorescence in isolated spinach chloroplasts, Biochim. Biophys. Acta 120 (1966) 23–33.
[49] D. Lazar, Chlorophyll a fluorescence induction, Biochim. Biophys. Acta 1412 (1999) 1–28.
[50] P. Haldimann, M. Tsimilli-Michael, Mercury inhibits the non-photochemical reduction of plastoquinone by exogenous NADPH and NADH: evidence from measurements of the polyphasic chlorophyll a fluorescence rise in spinach chloroplasts, Photosynth. Res. 74 (2002) 37–50.
[51] A. Joliot, P. Joliot, Etudes cinetique de la reaction photochimique liberant l'oxygen au cours de la photosynthese, C. R. Acad. Sci. Paris Ser. D 278 (1964) 4622–4625.
[52] G. Paillotin, Movement of excitations in the photosynthetic domains of photosystem II, J. Theor. Biol. 58 (1976) 237–252.
[53] C. Vernotte, A.L. Etienne, J.M. Briantais, Quenching of the system II chlorophyll fluorescence by the plastoquinone pool, Biochim. Biophys. Acta 545 (1979) 519–527.
[54] J. Kurreck, R. Schödel, G. Renger, Investigation of the plastoquinone pool size and fluorescence quenching in thylakoid membranes and photosystem II (PS II) membrane fragments, Photosynth. Res. 63 (2000) 171–182.
[55] S.Z. Tóth, G. Schansker, R.J. Strasser, In intact leaves, the maximum fluorescence level (F(M)) is independent of the redox state of the plastoquinone pool: a DCMU-inhibition study, Biochim. Biophys. Acta 1708 (2005) 275–282.
[56] A. Hope, P. Valente, Inhibitor binding to isolated chloroplast cytochrome *bf* complex, Photosynth. Res. 49 (1996) 37–48.
[57] W.A. Cramer, H. Zhang, J. Yan, Binding sites of lipophilic quinone and quinone analogue inhibitors in the cytochrome b_6f complex of oxygenic photosynthesis, Biochem. Soc. Trans. 33 (2005) 921–923.
[58] J. Harbinson, C.L. Hedley, The kinetics of P-700$^+$ reduction in leaves: a novel in situ probe of thylakoid functioning, Plant Cell Environ. 12 (1989) 357–369.
[59] A. Hope, R.R. Huilgol, M. Panizza, M. Thompson, D.B. Matthews, The flash-induced turnover of cytochrome *b*-563, cytochrome *f*, and plastocyanin in chloroplasts. Models and estimation of kinetic parameters, Biochim. Biophys. Acta 1100 (1992) 15–26.
[60] R.E. Cleland, D.S. Bendall, Photosystem-I cyclic electron-transport — measurement of ferredoxin–plastoquinone reductase-activity, Photosynth. Res. 34 (1992) 409–418.
[61] K. Oxborough, P. Horton, Characterization of the effects of antimycin-a upon high-energy state quenching of chlorophyll fluorescence (qE) in spinach and pea-chloroplasts, Photosynth. Res. 12 (1987) 119–128.
[62] P. Horton, A.V. Ruban, D. Rees, A.A. Pascal, G. Noctor, A.J. Young, Control of the light-harvesting function of chloroplast membranes by aggregation of the LHCII chlorophyll–protein complex, FEBS Lett. 292 (1991) 1–4.
[63] A.R. Crofts, C.T. Yerkes, A molecular mechanism for qE-quenching, FEBS Lett. 352 (1994) 265–270.
[64] C.T. Yerkes, A.R. Crofts, The quenching of fluorescence in PSII by delta pH: dependence on the state of the oxygen evolving complex, and effects of antimycin, in: N. Murata (Ed.), Research on Photosynthesis, Kluwer Academic Publishers, Netherlands, 1992, pp. 635–638.
[65] W.A. Cramer, H. Böhme, High-potential cytochrome b-559 as a secondary quencher of chloroplast fluorescence in the presence of 3-(3, 4-dichlorophenyl)-1, 1-dimethylurea, Biochim. Biophys. Acta 256 (1972) 358–369.
[66] C. Miyake, U. Schreiber, K. Asada, Ferredoxin-dependent and antimycin a-sensitive reduction of cytochrome b-559 by far-red light in maize thylakoids; participation of a menadiol-reducible cytochrome b-559 in cyclic electron flow, Plant Cell Physiol. 36 (1995) 743–748.
[67] W.A. Cramer, W.L. Butler, Potentiometric titration of the fluorescence yield of spinach chloroplasts, Biochim. Biophys. Acta 172 (1969) 503–510.
[68] A. Krieger, A.W. Rutherford, G.N. Johnson, On the determination of redox midpoint potential of the primary quinone electron acceptor, Q_A, in photosystem II, Biochim. Biophys. Acta 1229 (1995) 193–201.
[69] T. Shibamoto, Y. Kato, R. Nagao, T. Yamazaki, T. Tomo, T. Watanabe, Species-dependence of the redox potential of the primary quinone electron acceptor Q_A in photosystem II verified by spectroelectrochemistry, FEBS Lett. 584 (2010) 1526–1530.
[70] K.K. Karukstis, S.C. Boegeman, J.A. Fruetel, S.M. Gruber, M.H. Terris, Multivariate analysis of photosystem II fluorescence quenching by substituted benzoquinones and naphthoquinones, Biochim. Biophys. Acta 891 (1987) 256–264.
[71] A.W. Rutherford, P. Mathis, A relationship between the midpoint potential of the primary acceptor and low temperature photochemistry in photosystem II, FEBS Lett. 154 (1983) 328–334.
[72] A. Krieger-Liszkay, A.W. Rutherford, Influence of herbicide binding on the redox potential of the quinone acceptor in photosystem II: relevance to photodamage and phytotoxicity, Biochemistry 37 (1998) 17339–17344.
[73] G.N. Johnson, A.W. Rutherford, A. Krieger, A change in the midpoint potential of the quinone Q_A in photosystem II associated with photoactivation of oxygen evolution, Biochim. Biophys. Acta 1229 (1995) 202–207.
[74] K. Ido, C.M. Gross, F. Guerrero, A. Sedoud, T.-L. Lai, K. Ifuku, A.W. Rutherford, A. Krieger-Liszkay, High and low potential forms of the Q_A quinone electron acceptor in photosystem II of *Thermosynechococcus elongatus* and spinach, J. Photochem. Photobiol. B 104 (2011) 154–157.
[75] A. Krieger, E. Weis, S. Demeter, Low-pH-induced Ca^{2+} ion release in the water-splitting system is accompanied by a shift in the midpoint redox potential of the primary quinone acceptor QA, Biochim. Biophys. Acta 1144 (1993) 411–418.
[76] C. Fufezan, C.M. Gross, M. Sjodin, A.W. Rutherford, A. Krieger-Liszkay, D. Kirilovsky, Influence of the redox potential of the primary quinone electron acceptor on photoinhibition in photosystem II, J. Biol. Chem. 282 (2007) 12492–12502.
[77] H. Ishikita, E.-W. Knapp, Control of quinone redox potentials in photosystem II: electron transfer and photoprotection, J. Am. Chem. Soc. 127 (2005) 14714–14720.
[78] E.-M. Aro, M. Suorsa, A. Rokka, Y. Allahverdiyeva, V. Paakkarinen, A. Saleem, N. Battchikova, E. Rintamäki, Dynamics of photosystem II: a proteomic approach to thylakoid protein complexes, J. Exp. Bot. 56 (2005) 347–356.
[79] W. Vredenberg, V. Kasalicky, M. Durchan, O. Prasil, The chlorophyll a fluorescence induction pattern in chloroplasts upon repetitive single turnover excitations: accumulation and function of Q_B-nonreducing centers, Biochim. Biophys. Acta 1757 (2006) 173–181.
[80] G. Schansker, R.J. Strasser, Quantification of non-Q_B-reducing centers in leaves using a far-red pre-illumination, Photosynth. Res. 84 (2005) 145–151.
[81] Y. Umena, K. Kawakami, J.-R. Shen, N. Kamiya, Crystal structure of oxygen-evolving photosystem II at a resolution of 1.9 Å, Nature 473 (2011) 55–60.
[82] K. Haussühl, B. Andersson, I. Adamska, A chloroplast DegP2 protease performs the primary cleavage of the photodamaged D1 protein in plant photosystem II, EMBO J. 20 (2001) 713–722.
[83] S. Bailey, E. Thompson, P.J. Nixon, P. Horton, C.W. Mullineaux, C. Robinson, N.H. Mann, A critical role for the Var2 FtsH homologue of *Arabidopsis thaliana* in the photosystem II repair cycle in vivo, J. Biol. Chem. 277 (2002) 2006–2011.
[84] C.C. Moser, J.M. Keske, K. Warncke, R.S. Farid, P.L. Dutton, Nature of biological electron transfer, Nature 355 (1992) 796–802.
[85] S. Itoh, Membrane surface potential and the reactivity of the system II primary electron acceptor to charged electron carriers in the medium, Biochim. Biophys. Acta 504 (1978) 324–340.
[86] D.F. Ghanotakis, G.T. Babcock, C.T. Yerkes, Exogenous versus endogenous acceptors in photosystem II in inhibited chloroplasts, Arch. Biochem. Biophys. 225 (1983) 248–255.
[87] S. Larom, F. Salama, G. Schuster, N. Adir, Engineering of an alternative electron transfer path in photosystem II, Proc. Natl. Acad. Sci. U. S. A. 107 (2010) 9650–9655.
[88] P. Zhang, M. Eisenhut, A.-M. Brandt, D. Carmel, H.M. Silén, I. Vass, Y. Allahverdiyeva, T.A. Salminen, E.-M. Aro, Operon flv4–flv2 provides cyanobacterial photosystem II with flexibility of electron transfer, Plant Cell 24 (2012) 1952–1971.
[89] P.J. Nixon, M. Barker, M. Boehm, R. de Vries, J. Komenda, FtsH-mediated repair of the photosystem II complex in response to light stress, J. Exp. Bot. 56 (2005) 357–363.
[90] J. Lavergne, J.-M. Briantais, Photosystem II heterogeneity, in: D. Ort, C. Yocum, I. Heichel (Eds.), Oxygenic Photosynthesis: The Light Reactions, Springer, Netherlands, 1996, pp. 265–287.
[91] J. Barber, Influence of surface charges on thylakoid structure and function, Annu. Rev. Plant Physiol. 33 (1982) 261–295.
[92] A.W. Rutherford, A. Osyczka, F. Rappaport, Back-reactions, short-circuits, leaks and other energy wasteful reactions in biological electron transfer: redox tuning to survive life in O_2, FEBS Lett. 586 (2012) 603–616.
[93] J. Lavergne, F. Rappaport, Stabilization of charge separation and photochemical misses in photosystem II, Biochemistry 37 (1998) 7899–7906.
[94] F. Rappaport, M. Guergova-Kuras, P.J. Nixon, B.A. Diner, J. Lavergne, Kinetics and pathways of charge recombination in photosystem II, Biochemistry 41 (2002) 8518–8527.
[95] H. Conjeaud, P. Mathis, The effects of pH on the reductions kinetics of P-680 in Tris-treated chloroplasts, Biochim. Biophys. Acta 590 (1980) 353–359.
[96] C.A. Tracewell, G.W. Brudvig, Two redox-active β-carotene molecules in photosystem II, Biochemistry 42 (2003) 9127–9136.
[97] V.V. Klimov, V.A. Shuvalov, U. Heber, Photoreduction of pheophytin as a result of electron donation from the water-splitting system to photosystem-II reaction centers, Biochim. Biophys. Acta 809 (1985) 345–350.
[98] J.M. Hou, V.A. Boichenko, B.A. Diner, D. Mauzerall, Thermodynamics of electron transfer in oxygenic photosynthetic reaction centers: volume change, enthalpy, and entropy of electron-transfer reactions in manganese-depleted photosystem II core complexes, Biochemistry 40 (2001) 7117–7125.
[99] C.A. Buser, L.K. Thompson, B.A. Diner, G.W. Brudvig, Electron-transfer reactions in manganese-depleted photosystem II, Biochemistry 29 (1990) 8977–8985.
[100] A.K. Livingston, J.A. Cruz, K. Kohzuma, A. Dhingra, D.M. Kramer, An *Arabidopsis* mutant with high cyclic electron flow around photosystem I (hcef) involving the NADPH dehydrogenase complex, Plant Cell 22 (2010) 221–233.
[101] Y. Okegawa, T.A. Long, M. Iwano, S. Takayama, Y. Kobayashi, S.F. Covert, T. Shikanai, A balanced PGR5 level is required for chloroplast development and optimum operation of cyclic electron transport around photosystem I, Plant Cell Physiol. 48 (2007) 1462–1471.